Contactless Inductive Technique for Electrical Conductivity Measurements on Molten Metals[1]

S. G. Teodorescu[2], R. A. Overfelt[2] and S. I. Bakhtiyarov[2,3]

---

[1] Paper presented at the Fourteenth Symposium on Thermophysical Properties, June 25-30, 2000, Boulder, Colorado, U.S.A.

[2] Department of Mechanical Engineering, 201 Ross Hall, Auburn University, AL 36849-5341, U.S.A.

[3] To whom correspondence should be addressed.

ABSTRACT

A computer controlled rotational technique to measure the electrical resistivity of solid and molten metals has been developed. The electrical resistivity of pure metals (aluminum, indium, lead and tin) and low melting point alloy LMA-158 at solid and liquid states was measured. The results also show that there is a linear relationship between electrical resistivity and temperature at both solid and liquid states of the test materials. A good agreement was found between our experimental data and predictions known from the literature. The data were used to estimate the temperature coefficients of electrical resistivity of test specimens over a wide range of temperatures including the melting point of the metals. A good agreement between experimental data and predictions made by previous researchers has been achieved.

KEY WORDS: electrical conductivity; molten metal; inductive method; lead; tin; aluminum.

1. INTRODUCTION

The optimization and control of metallurgical processes requires the knowledge of many physical properties (e.g., viscosity, electrical conductivity, density, surface tension) of metals in the liquid state. Electrical conductivity is a basic physical factor in evaluation and designing new alloys, and provides valuable information about the structure of molten metals in many metallurgical processes such as electroslug remelting and electromagnetic stirring in continuous and centrifugal castings.

By virtue of a disordered arrangement of ions the metals in liquid state have higher (~ 1.5 - 2.3 times) electrical resistivity than solid metals with regular arrangement of ions. The decrease in electrical conductivity is caused by the shortening the electron mean free path when they are moving through the disordered liquid state [1]. The vibrating atoms model [2], the free-electron model [3,4] and the fluctuation scattering theory [5,6] are three main theories, which allow predicting an electrical conductivity of molten metals. Electrical conductivity predicted by these theories is in good agreement with experimental data obtained by different researchers.

Braunbeck [7] proposed the following relationship between the electric conductivity of the specimen and the mechanical moment caused by mutual interaction between the external magnetic field and an additional magnetic field induced by the eddy current:

$$M = \frac{\pi}{4}\sigma_e\ \omega\ L\ R^4\ B^2 - \frac{\pi}{192\,\eta}\sigma_e^2\ \omega\ L\ R^6\ B^4, \qquad (1)$$

where M is the mechanical moment caused by mutual interaction between the external magnetic field and an additional magnetic field induced by the eddy current; L and R are length and radius of the specimen, respectively; ω is the angular velocity of the rotating magnetic field; B is the magnetic induction; η is the viscosity of the liquid specimen.

According to [8], the magnetic induction and the dimension of the specimen can be selected so that the second term in equation (1) may become negligibly small compared with the first term in the case of metals of unknown viscosity.

The methods of electrical conductivity measurements can be categorized into two groups:

- direct resistance measurements and
- contactless inductive measurements.

In direct resistance measurement techniques high melting noble metals (platinum, molybdenum, etc.) are used as electrodes. In aggressive metal melts they are subject to solution attack. Therefore, these methods are applicable for poor conductors and for calibration of the contactless inductive technique.

As a direct technique, four-probe potentiometric method has been developed to measure electrical conductivity of molten metals [9,10]. In this method, at a constant current density the potential drop across the molten sample in a capillary tube of a known cross-section and length is measured. The probe cell has to be calibrated using a liquid metal (usually mercury) of known electrical conductivity. A selection of the proper material for the capillary cell and the electrodes is a main problem in this method. Dissolution of electrodes and chemical reaction between them may happen. Hence, an

improved four-probe method has been developed later [11]. This method uses solid electrodes made of identical material to the molten sample.

The contactless inductive measurement technique excludes the dissolution, chemical reaction and contact resistance phenomena. The method is based on the phenomena that when a metal sample moves in a magnetic field (or magnetic field rotates around the sample), circulating eddy currents are induced in the sample. These currents generate a damping torque proportional to the electrical conductivity of the sample. In liquid metals and alloys the applied magnetic field causes the liquid circulation in the crucible. Consequently, it results in a decrease in the velocity of induced eddy currents. The rotating magnetic field method to measure the electrical conductivity of molten metals and alloys has been used by [12-14]. The advantage of the method is the possibility of measuring at the same time the viscosity of the molten sample by the damping of the torsional oscillation of the cell [15].

The capillary technique has been in [16,17] to measure the electric conductivity of the lead-tin binary system. The rotational technique was used in [18-20]. There is good agreement between the data obtained by rotational techniques. However, the data obtained by the capillary techniques are disagreed among themselves and with data obtained by rotational methods. Ozelton and Wilson [20] assume that the capillary method is affected by the separation of the constituents (liquid and solid) of the alloy by the direct electric current passage.

The objective of this work is to design a contactless inductive technique (with a metal sample moving in a magnetic field) for measuring the electrical resistivity of solid

and liquid metals. This paper presents some preliminary results for pure metals and low melting point alloy over a wide range of temperatures.

2. TEST MATERIALS, EXPERIMENTAL APPARATUS AND PROCEDURE

Schematics of the experimental set ups to measure an electrical conductivity of metals and alloys at high temperatures are illustrated in Figures 1 and 2. Computer controlled Brookfield rheometer Model DV-III has been used to provide a constant rotational speed to metal sample and to measure the torque precisely. This rheometer allows to make torque measurements (0 to 673.7 dyne-cm) at constant speeds from 0 to 250 RPM in 0.1 RPM increments. Rheometer has RS232 Compatible serial Port for use with attached PC.

The temperature of the sample has been measured simultaneously by three thermocouples. Temperature probe DVP-28Y was connected to computer and data obtained were synchronized with data for measured torque and angular velocity of crucible. The outputs of other two thermocouples were coupled to Digital Temperature Indicator. The thermocouples have been calibrated against the melting points of pure lead and tin. In addition, Micron Infrared Thermometer has been used to measure the temperature at crucible surface.

The metal sample was placed inside the flat-bottomed cylindrical, extruded, high purity alumina crucible attached to the spindle of the rheometer through a specially designed coupling system to provide a concentricity to the rotating crucible with sample. The alumina crucibles (9.525 mm diameter and 152.4 mm length) with the samples of the same diameter and 38.1 mm length have been exposed to magnetic field and heating.

During each set of tests it was essential to maintain sample length constant. For each metal sample the mass has been determined according to the required size of sample and density.

The motor driven 3D positioning system has been designed and fabricated to provide a high accuracy positioning to the crucible with the sample, heating elements, magnets and infrared thermometer. Gear motor with maximum speed 500 RPM was used in the positioning system to provide low speed variations (0.1%).

A quartz infrared line heating elements housed in an elliptical cast aluminum frames have been used as a furnace in the experimental apparatus depicted in Figure 1. The heated length of the chamber is 167 mm. The elliptical reflectors provide concentrated infrared energy to the test specimen. High-density infrared energy is produced by tubular, high temperature quartz lamps (Q2000T4/CL) with tungsten wire filament emitters. The lamps supply energy (2 kW each) in the infrared region above the visible range in the electromagnetic spectrum and are housed in an array of elliptical reflectors. The reflectors focus infrared energy from the lamps on the specimen (Figure 3). The full voltage temperature output is 2980^{o} C. Copper tube connections are provided for inlet and outlet flow of coolant (water) to cool lamp reflector bodies. Tap water at 15^{o} C and 600 kPa was supplied to cool the unit.

In experimental technique presented in Figure 2, a paraboloidal reflector was used to capture the light sent by the 5 kW Xenon lamp coated with bright rhodium. The light was focused into the point located 60 mm below the top. The auto-shutting off relay was incorporated inside the power supply and allowed to heat the sample ~ 10 min. The internal blower cooled the lamp.

The magnetic field has been generated by two neodymium permanent magnets. MG-4D gaussmeter (Walker Scientific Inc.) operated on the Hall-effect principle has been used to measure the magnetic field strength. It provides DC and AC field readings from $\pm 10^{-5}$ T to $\pm$ 2 T with 0.1% resolution. Changing the distance between the magnets we could obtain a magnetic field of desirable strength. It was significant to obtain a magnetic field with uniformly distributed induction. Mapping performed by MG-4D gaussmeter revealed that the magnetic induction varies in both vertical and horizontal directions. Contour lines for the magnetic induction at different distances between the magnets are shown in Figure 4. Estimations indicate that the magnetic induction over the test sample varies ±10% in vertical direction and ±7% in horizontal direction compared to its average value. Figure 5 shows the variation of the magnetic induction with the distance between the magnets. Neither the coupling system nor the alumina crucible had perceptible disturbing effects upon the applied magnetic field.

As a test sample we used aluminum of 99.999% purity, indium (99.99%), lead (99.9999%), tin (99.999%) and a low melting alloy LMA-158. The composition of this alloy and some thermo-physical properties of the components at liquid state are shown in Table 1. The electrical resistance of the solid samples also has been measured by using 4300B Digital Micro-ohmmeter (Valhalla Scientific, Inc.). The Kelvin four-terminal configuration of this ohmmeter eliminates errors caused by test lead and contact resistance that in many applications can exceed the value of the load by several orders of magnitude.

Table 1. LMA-158 components and their thermo-physical properties in liquid state [1].

LMA-158 components	Weight %	Melting Point ^{0}K	Density g / cm^3	Electrical Resistivity	Viscosity mPa-s
Bismuth	50.0	544.1	10.05	130.2	1.63
Lead	26.7	600.55	10.67	95	2.61
Tin	13.3	504.99	6.98	48	1.81
Cadmium	10.0	594.05	8.01	33.7	2.60

3. RESULTS AND DISCUSSION

The effect of the induced magnetic field is characterized by the magnetic Reynolds number defined as

$$\mathrm{Re}_m = \omega\, \sigma_e\, \mu_0\, R^2\,, \tag{2}$$

where μ_0 is magnetic permeability. Simulations show that in our experiments $Re_m \ll 1$, which means that the magnetic field distribution is not affected by the fluid motion and may be evaluated as though the conducting liquid were a solid. Also, the induction of an electric field by fluctuations of the magnetic field can be disregarded in comparison with the electromagnetic force.

The flow regime of the melt flow in rotating cylindrical container is determined by hydraulic Reynolds number, which represents the ratio of inertia forces to viscous forces, and is defined by the formula

$$\mathrm{Re} = \frac{\omega R^2 \rho}{\mu}, \tag{3}$$

where μ and ρ are shear viscosity and density of the liquid metal, respectively, ω is an angular velocity of fluid rotation. The calculations of the Reynolds for lead, tin and aluminum at test conditions show the flow regime in container for all samples are laminar.

First, the damping torque has been calibrated against the electrical resistivity of pure lead and tin. The damping torque, hence electrical resistivity increases with increasing the sample length. Then, one would assume a significant contribution of end effects on the measured values of damping torque. The effects can be eliminated from the results of two experiments accomplished with different heights (24.5 mm and 36.75 mm) of the test sample in the crucible but at the same angular speed (ω = 35 RPM) and diameter (19.2 mm). Calibration results with elimination of the end effects are shown in Figures 6 and 7 along with simulation results by formula (1) for lead and tin, respectively. As seen from these figures, there is a good agreement between calibration data and predictions.

The variation of the damping torque, caused by the induced circular eddy currents, for aluminum, indium, lead and tin samples, with the angular velocity at different temperatures is shown in Figure 8. As seen from this figure, damping torque decreases with temperature at fixed angular speed (ω = 35 RPM) and magnetic induction (B = 0.1 T). As seen from this figure, at melting points of the test samples the torque dramatically decreases as a result of weak eddy currents for samples in liquid phase.

Figure 9 represents a variation of the electrical resistivity of the test samples in both solid and liquid states against temperature. The data are in good agreement with ones known from the literature.

The electrical resistivity of LMA-158 alloy as a function of temperature is represented in Figure 10. As seen from the figure, at melting point (T = 70 ^{0}C) of the alloy the electrical resistivity increases almost twice. The results also show that there is a linear relationship between electrical resistivity and temperature at both solid and liquid states of the alloy.

It is well known that the change of electrical resistance of conductor materials in both solid and liquid phases is proportional to the change of temperature. The electrical resistivity of liquid metals increases linearly with increasing temperature (except for Cd and Zn) [1]. This relationship can be expressed as

$$\rho_e = \alpha T + \beta \,, \tag{4}$$

where α and β are temperature coefficients of the electrical resistivity for liquid metals.

The measured values of the temperature coefficients (α and β) of resistivity for molten aluminum, indium, lead, tin and LMA-158 alloy samples at different temperatures are presented in Figures 11 and 12. The lines denote the values of these coefficients proposed in [21]. As one would notice, there is an adequate agreement between the measured and proposed values of both temperature coefficients (with deviation $\pm$ 5%).

4. CONCLUSIONS

A contactless inductive rotational technique to measure the electrical resistivity of solid and molten metals has been developed. The furnaces with the elliptical and paraboloidal reflectors have been used to melt the metal samples. The damping torque was calibrated against the electrical resistivity of pure lead and tin. The end effects were eliminated from the results of two experiments accomplished with different lengths of the test sample in the crucible but with the same angular speed and sample diameter. The electrical resistivity of the pure metals (aluminum, indium, lead and tin) and low melting point alloy LMA-158 at solid and liquid states was measured. The results show that there is a linear relationship between electrical resistivity and temperature at both solid and liquid states of the test materials. A good agreement was found between our experimental data and predictions by Braunbeck [7].

The data were used to estimate the temperature coefficients of electrical resistivity of test specimens over a wide range of temperatures including the melting point of the metals. A good agreement between experimental data and predictions by previous researchers has been achieved.

ACKNOWLEDGEMENTS

The authors gratefully acknowledge the financial support received from NASA's Office of Life and Microgravity Sciences and Applications under Cooperative Agreement No. NCC8-128.

REFERENCES

1. T. Iida and R. I. L. Guthrie, *The Physical Properties of Liquid Metals*. Clarendon Press, Oxford (1988).
2. N. F. Mott, *Proc. Roy. Soc.* A146: 465 (1934).
3. J. M. Ziman, *Phil. Mag*. 6: 1013 (1961).
4. R. Evans, D. A. Greenwood and P. Lloyd, *Phys. Letters*. 35A: 57 (1971).
5. S. Takeuchi and H. Endo, *J. Japan Inst. Metals*. 26: 498 (1962).
6. J. L Tomlinson, and B. D. Lichter, *Trans. Met. Soc. AIME*. 245: 2261 (1969).
7. W. Braunbeck, Z. Phys. 3: 312 (1932).
8. S. Takeuchi and H. Endo, *Trans. Japan Inst. Metals*. 3: 30 (1962).
9. P. D. Adams and J. S. Leach, *Physical Reviews*. 156: 178 (1967).
10. Y. Mera, Y. Kita and A. Adachi, *Technology Reports of Osaka University*. 22: 445 (1972).
11. G. S. Ershov, A. A. Kasatkin, and I. V. Gavrilin, *Izv. Akad. Nauk SSSR. Metally*. 2: 98 (1976).
12. A. M. Samarin, *Journal of Iron and Steel Institute*. 200: 95 (1962).
13. Y. Ono and T. Yagi, *Transactions of ISIJ*. 12: 314 (1972).
14. S. I. Bakhtiyarov and R. A. Overfelt, *Journal of Materials Science*. 34: 945 (1999).
15. S. I. Bakhtiyarov and R. A. Overfelt, *Acta Materialia*. 47: 4311 (1999).
16. T. C. Toye and E. E. Jones, *Proc. Phys. Soc*. 71: 88 (1958).
17. A. M. Korolkov and D. P. Shashkov, *Izv. Akad. Nauk. SSSR, Met. i Topl*. 1: 84 (1962).
18. A. Roll and G. Fees, *Z. Metall*. 51: 540 (1960).

19. S. Takeuchi and H. Endo, *Trans. Japan Inst. Metals*: 3: 35 (1962).

20. M. W. Ozelton and J. R. Wilson, *J. Sci. Instrum*. 43: 359 (1966).

21. N. Cusack and J. E. Enderby, *Proc. Phys. Soc*. 75: 395 (1960).

FIGURE CAPTIONS

Fig. 1. Experimental apparatus used for electrical conductivity measurements of solid and molten metals.

Fig. 2. Experimental apparatus with paraboloidal reflector furnace used for electrical conductivity measurements of solid and molten metals.

Fig. 3. Diagram of sample-magnetic field-optical furnace arrangement and heating energy focus action.

Fig. 4. Contour lines for magnetic induction (in 10^4 T) at different distances between magnets: (a) 12 cm; (b) 9 cm; (c) 8 cm; (d) 7 cm.

Fig. 5. Variation of averaged magnetic induction with distance between magnets.

Fig. 6. Fig. 6. Calibration of damping torque for liquid lead at ω = 35 RPM, B= 0.1 T. Solid lines correspond to simulations by formula (1).

Fig. 7. Calibration of damping torque for liquid tin at ω = 35 RPM, B= 0.1 T. Solid lines correspond to simulations by formula (1).

Fig. 8. Variation of damping torque with temperature for aluminum, indium, lead and tin in solid and liquid states (ω = 35 RPM and B = 0.1 T).

Fig. 9. Variation of electrical resistivity with temperature for aluminum, indium, lead and tin in solid and liquid states (ω = 35 RPM and B = 0.1 T).

Fig. 10. Variation of electrical resistivity of LMA-158 alloy with temperature at ω = 35 RPM and B = 0.1 T.

Fig. 11. Variation of temperature coefficient α with temperature for liquid aluminum, indium, lead, tin and LMA-158 alloy (ω = 35 RPM and B = 0.1 T). Lines denote predictions by [21].

Fig. 12. Variation of temperature coefficient β with temperature for liquid aluminum, indium, lead, tin and LMA-158 alloy (ω = 35 RPM and B = 0.1 T). Lines denote predictions by [21].

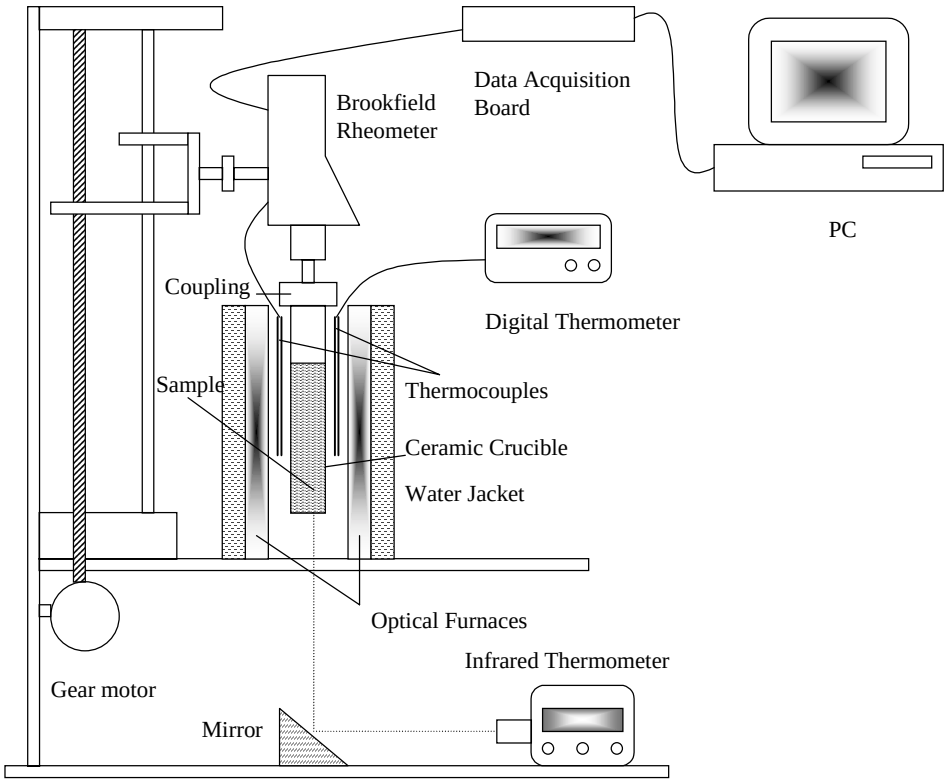

Fig. 1. Experimental apparatus used for electrical conductivity measurements of solid and molten metals.

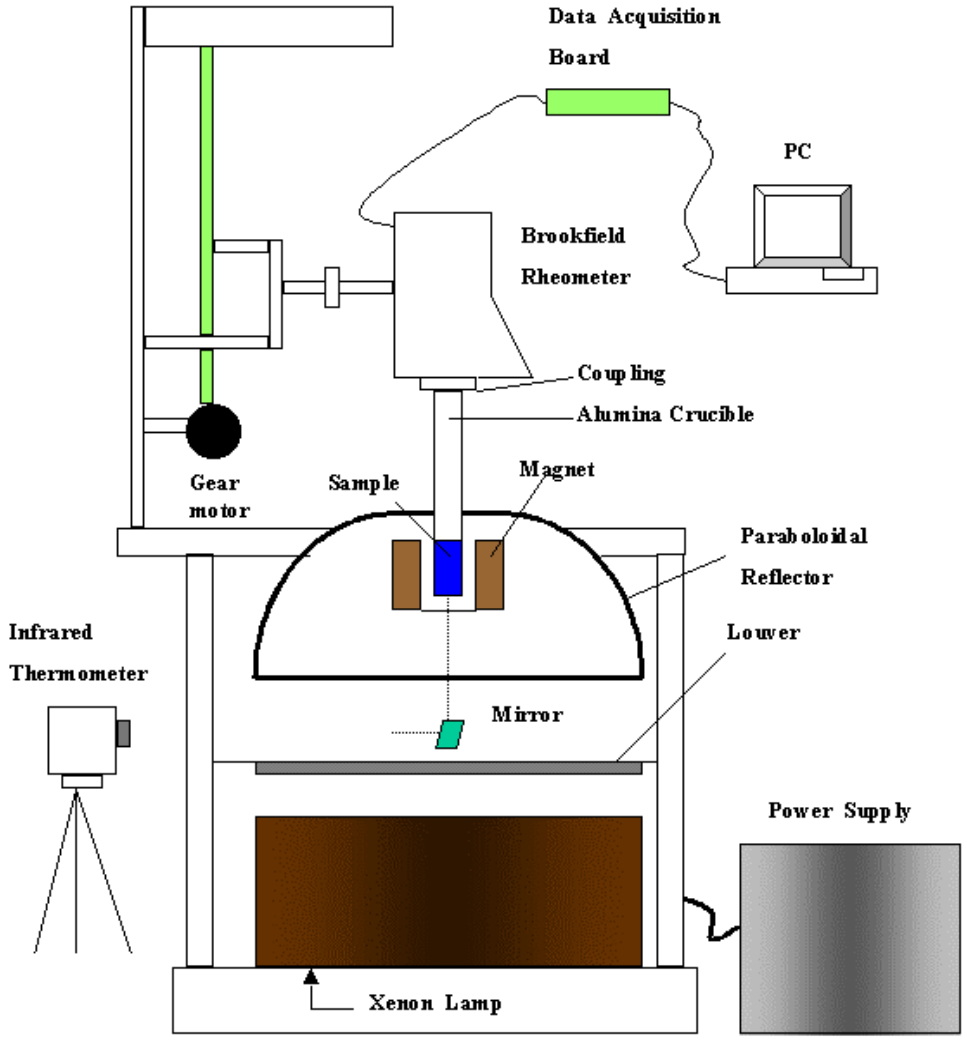

Fig. 2. Experimental apparatus with paraboloidal reflector furnace used for electrical conductivity measurements of solid and molten metals.

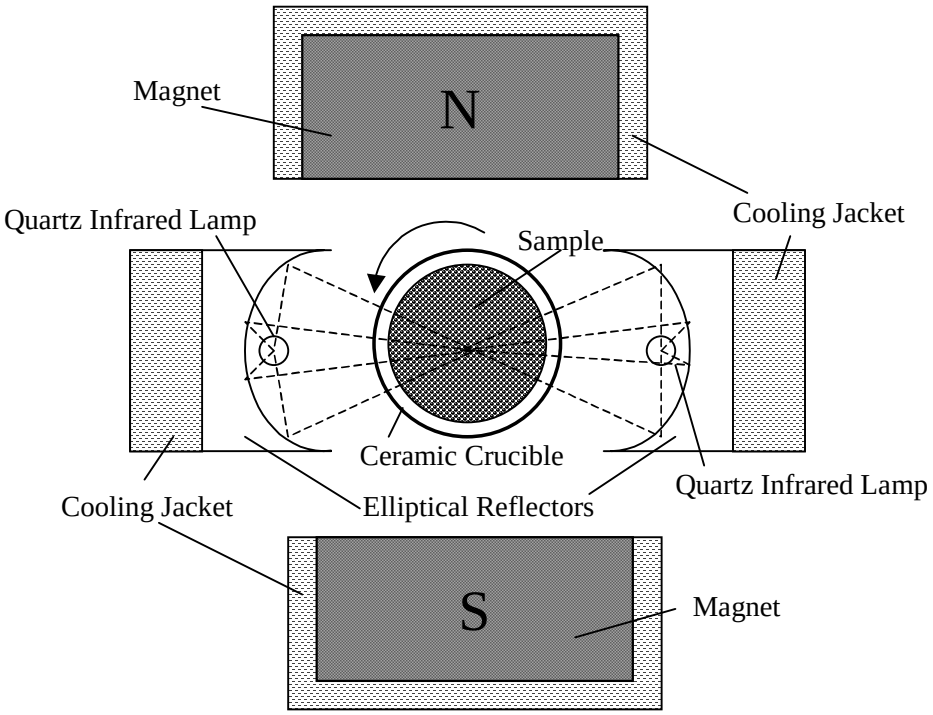

Fig. 3. Diagram of sample-magnetic field-optical furnace arrangement and heating energy focus action.

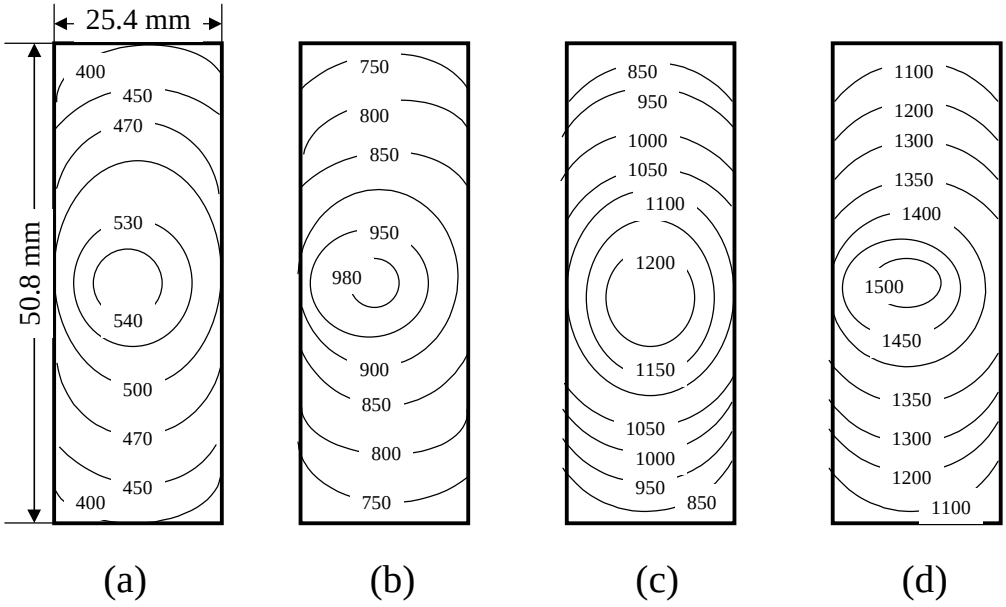

Fig. 4. Contour lines for magnetic induction (in 10^4 T) at different distances between magnets: (a) 12 cm; (b) 9 cm; (c) 8 cm; (d) 7 cm.

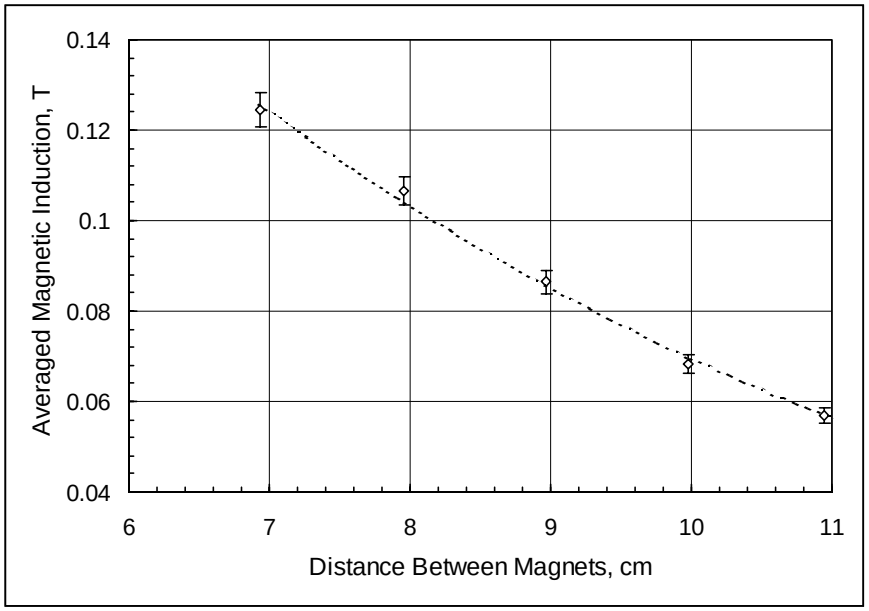

Fig. 5. Variation of averaged magnetic induction with distance between magnets.

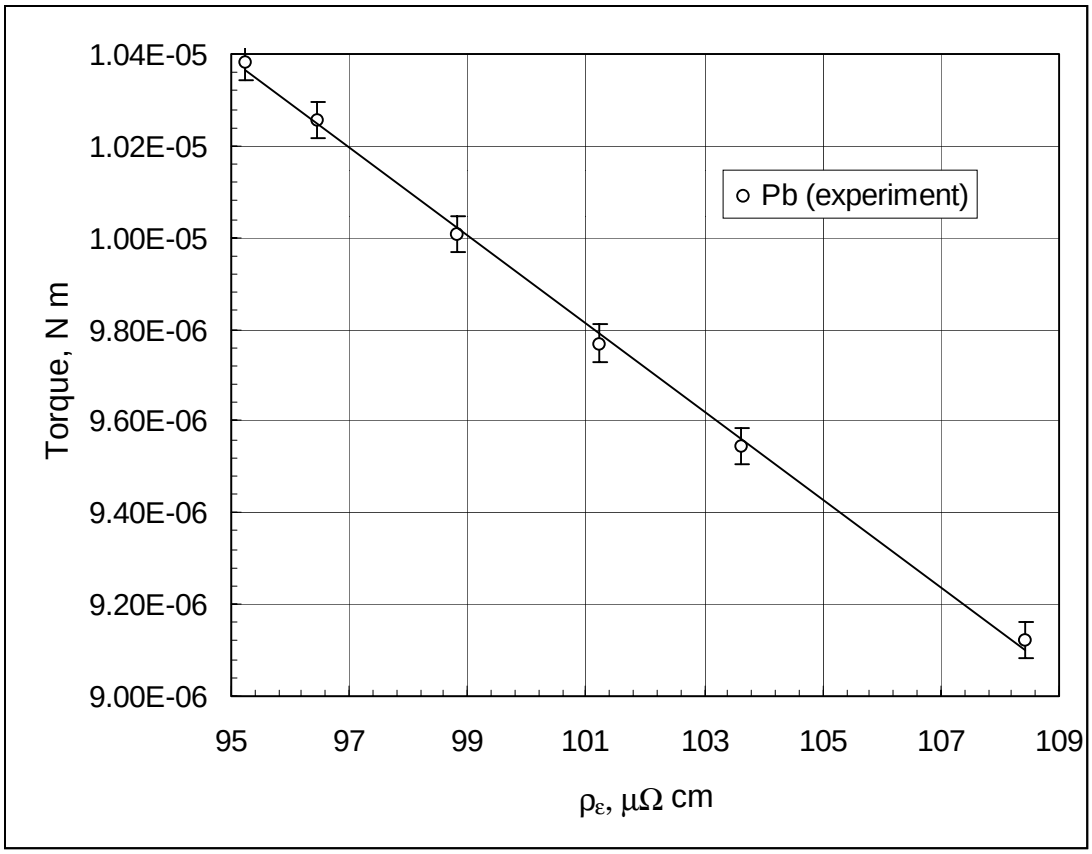

Fig. 6. Calibration of damping torque for liquid lead at $\omega = 35$ RPM, B= 0.1 T. Solid lines correspond to simulations by formula (1).

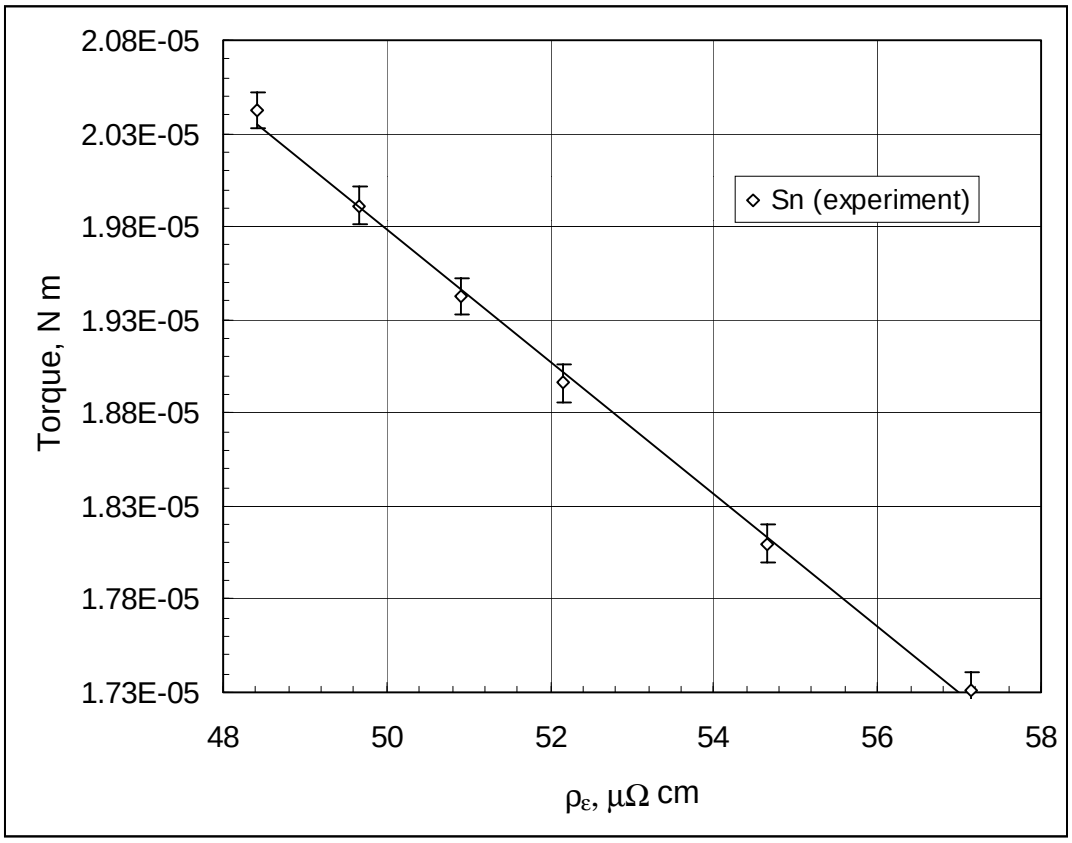

Fig. 7. Calibration of damping torque for liquid tin at ω = 35 RPM, B= 0.1 T. Solid lines correspond to simulations by formula (1).

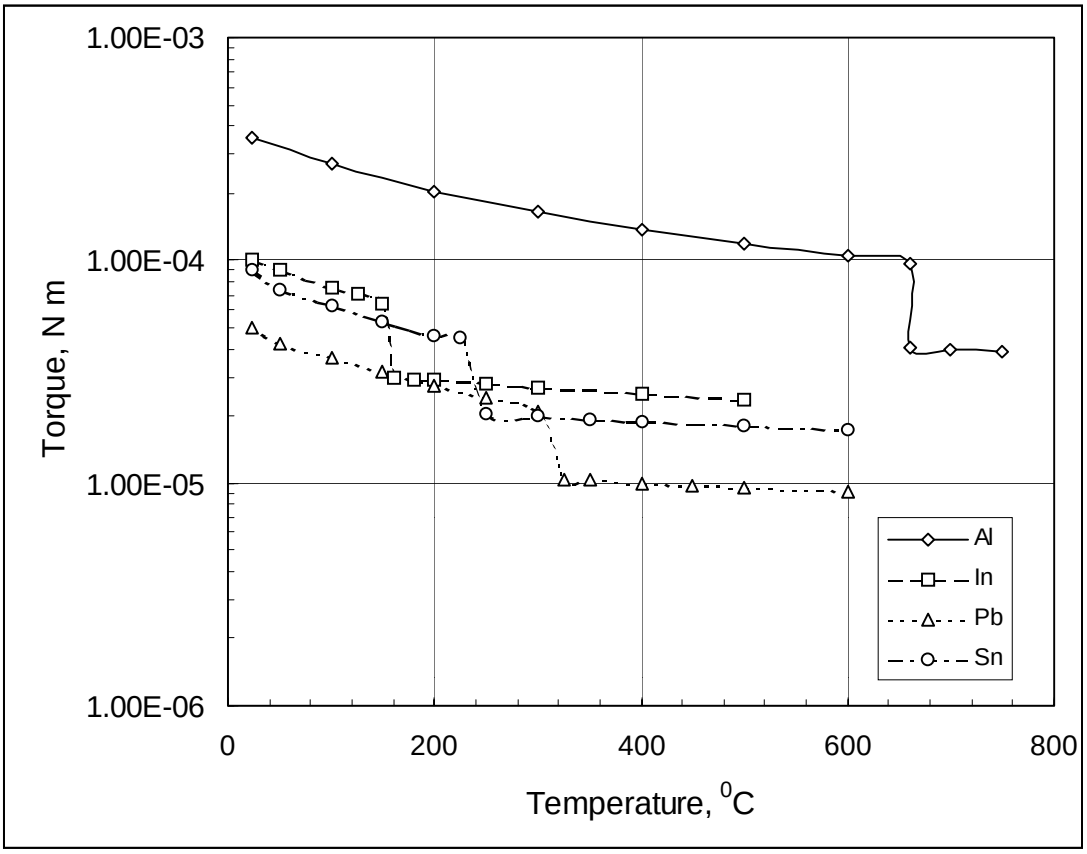

Fig. 8. Variation of damping torque with temperature for aluminum, indium, lead and tin in solid and liquid states (ω = 35 RPM and B = 0.1 T).

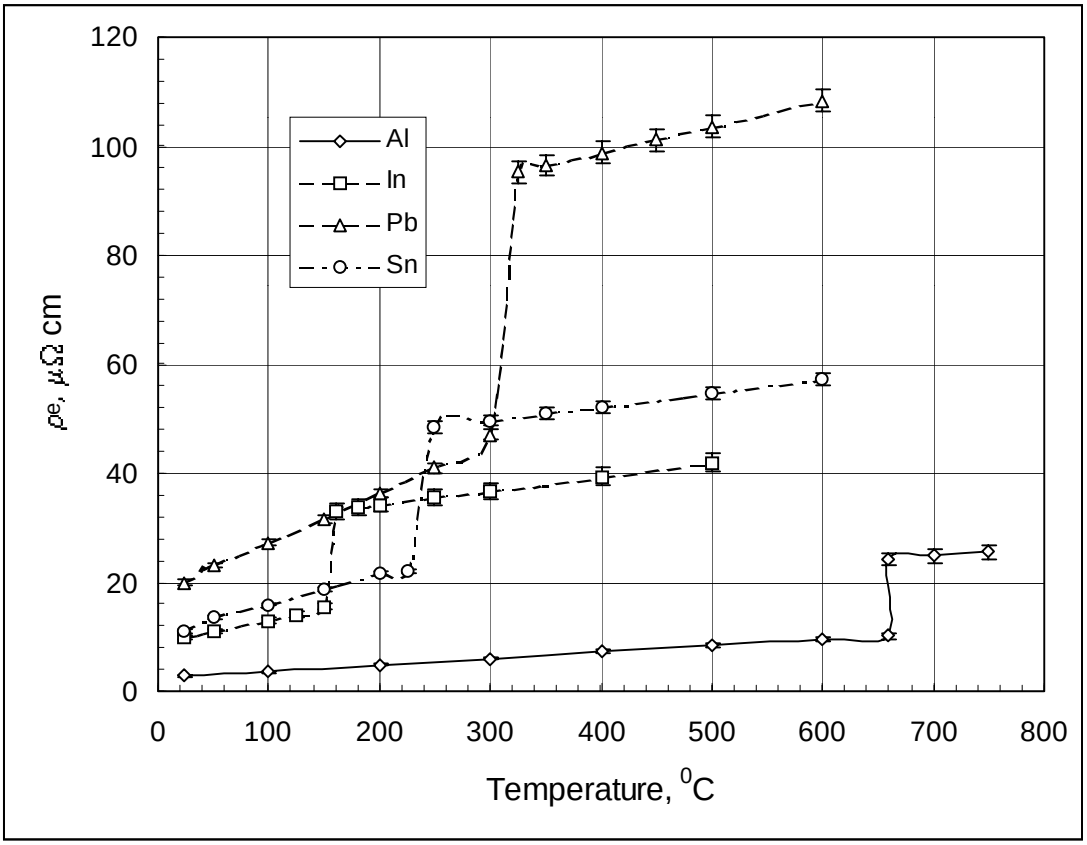

Fig. 9. Variation of electrical resistivity with temperature for aluminum, indium, lead and tin in solid and liquid states (ω = 35 RPM and B = 0.1 T).

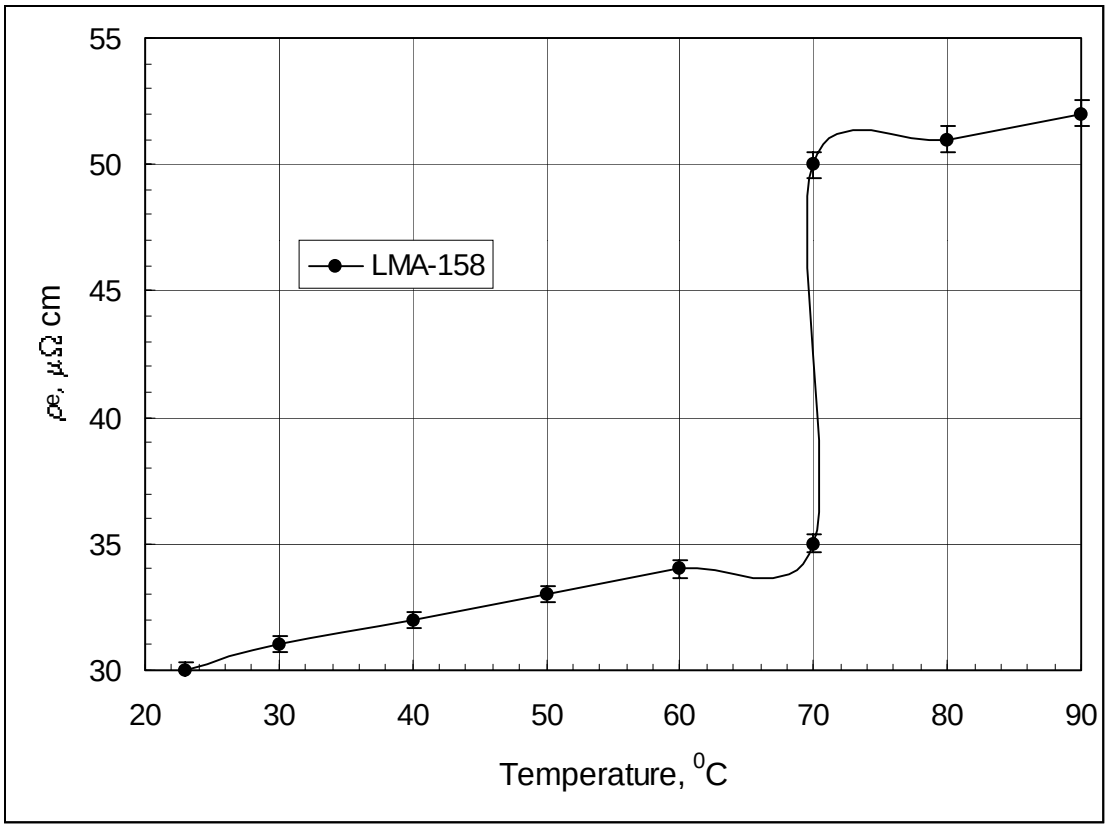

Fig. 10. Variation of electrical resistivity of LMA-158 alloy with temperature at ω = 35 RPM and B = 0.1 T.

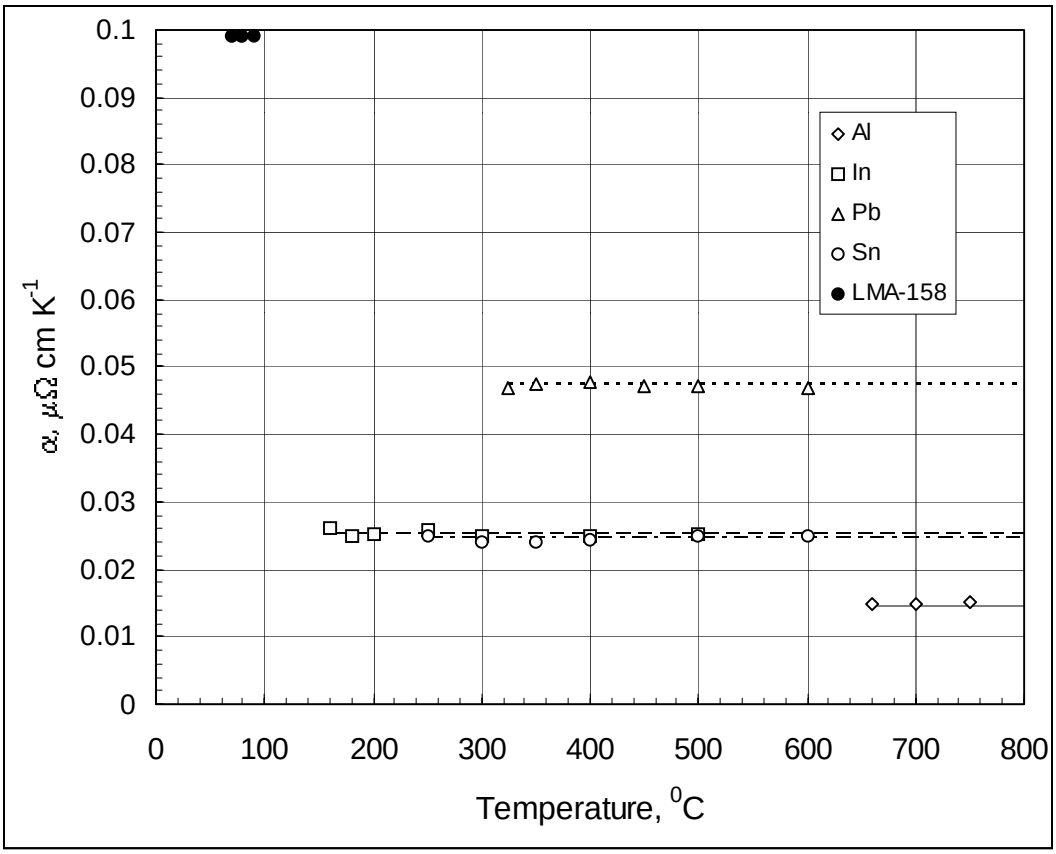

Fig. 11. Variation of temperature coefficient α with temperature for liquid aluminum, indium, lead, tin and LMA-158 alloy (ω = 35 RPM and B = 0.1 T). Lines denote predictions by [21].

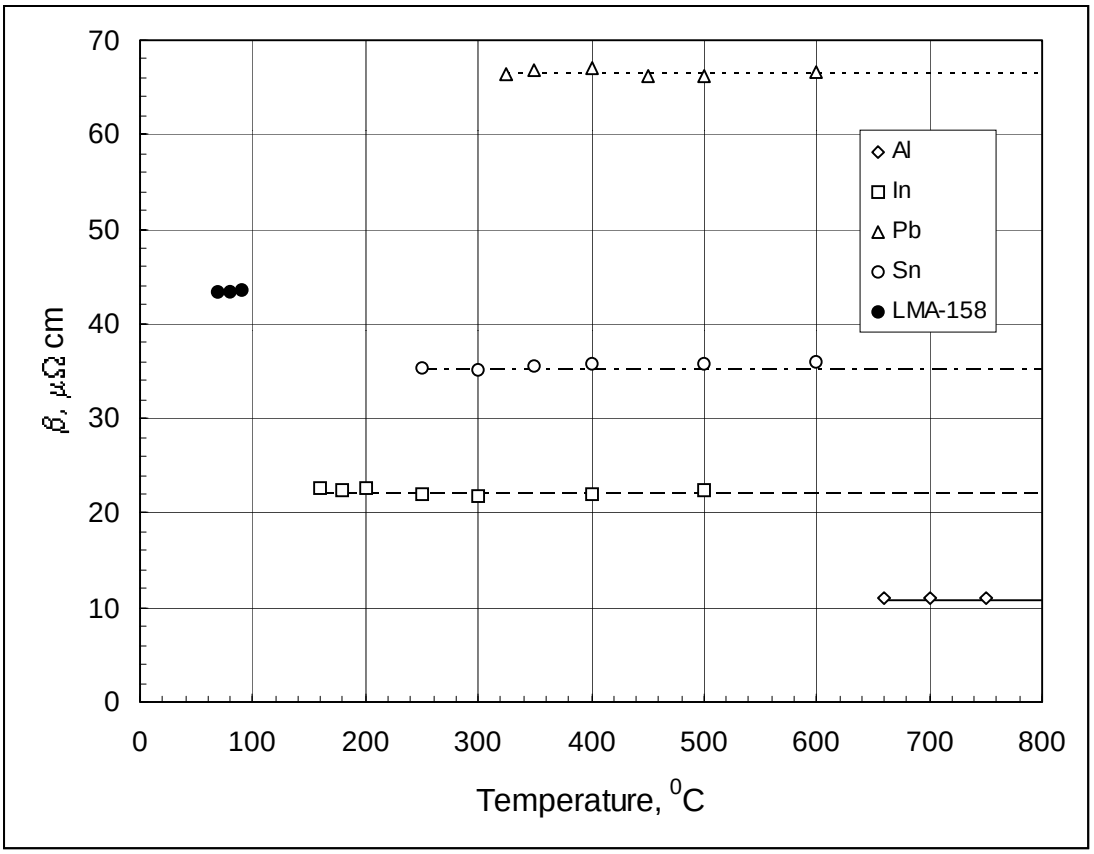

Fig. 12. Variation of temperature coefficient β with temperature for liquid aluminum, indium, lead, tin and LMA-158 alloy (ω = 35 RPM and B = 0.1 T). Lines denote predictions by [21].